JKAU: Eng. Sci., vol. 10 no. 2, pp. 77-91 (1418 A.H. / 1998 A.D.)

Criteria for Dynamic Flow Behavior below the Vibrating Sluice Gates

D. HUSAIN*, ABDEL-AZIM M. NEGM** and A.A. ALHAMID*
*Civil Eng. Dept., College of Eng., KSU, Riyadh, KSA
**Water and Water Str. Eng. Dept., Faculty of Eng.,
Zagazig University, Zagazig, Egypt.

ABSTRACT. This paper describes the results of experimental investigation on flow behavior below vibrating sluice gate models considering different gate bottom thicknesses. The pressure and force acting on gate bottom during underflow were measured. Based on Euler number variation on gate bottom, a criteria has been developed in terms of upstream head, gate opening ratio and gate bottom thickness for identifying the three cases of flow behavior below the gate as no-reattachment, stable reattachment and unstable reattachment. Depending upon the criteria, the pressure and force fluctuation data were analyzed in detail and the analysis revealed that both stable and unstable reattachment generate self excitation of the gate and consequently increases hydrodynamic loading significantly.

1. Introduction

Vertical lift sluice gates are commonly used for flow regulation and measurement in a variety of hydraulic structures. They operate mostly under conditions of underflow and the pulsations in flow underneath the gate is the major cause for gate vibrations[1-17]. These pulsations are the result of flow separation from the upstream edge of the gate bottom and subsequent reattachment at a certain downstream location. These separations and reattachment cause fluctuations in the pressure distribution underneath the gate and therefore the study of the pressure distribution – both mean and fluctuation components – at the gate bottom assumes importance for understanding the dynamic behavior below the gate. For gates with underflow, the separation and subsequent reattachment of flow with the gate bottom plays an important role in the hydrodynamic loading. It is therefore necessary to examine this flow pattern in more detail.

For high values of Reynold number, it is known that the configuration of the separation streamline is primarily a function of the geometry of boundaries[3,4,5,7]. In the present case of underflow with free water surface upstream and downstream of the gate,

eventually the boundaries are determined by the upstream water level, the gate opening and thickness and the downstream water level with respect to gate bottom. Thus in some cases, the separation streamline may go clearly off the gate bottom and eventually join downstream free water surface without attaching itself to the gate bottom. On the other hand, in some other cases it may reattach itself to the gate bottom[3,17]. If the location of the reattachment is far upstream of the trailing edge of the gate bottom (before the centre line), the reattachment is considered stable. For location near the trailing edge of the gate bottom, it is considered unstable. These are demonstrated schematically in Fig. 1.

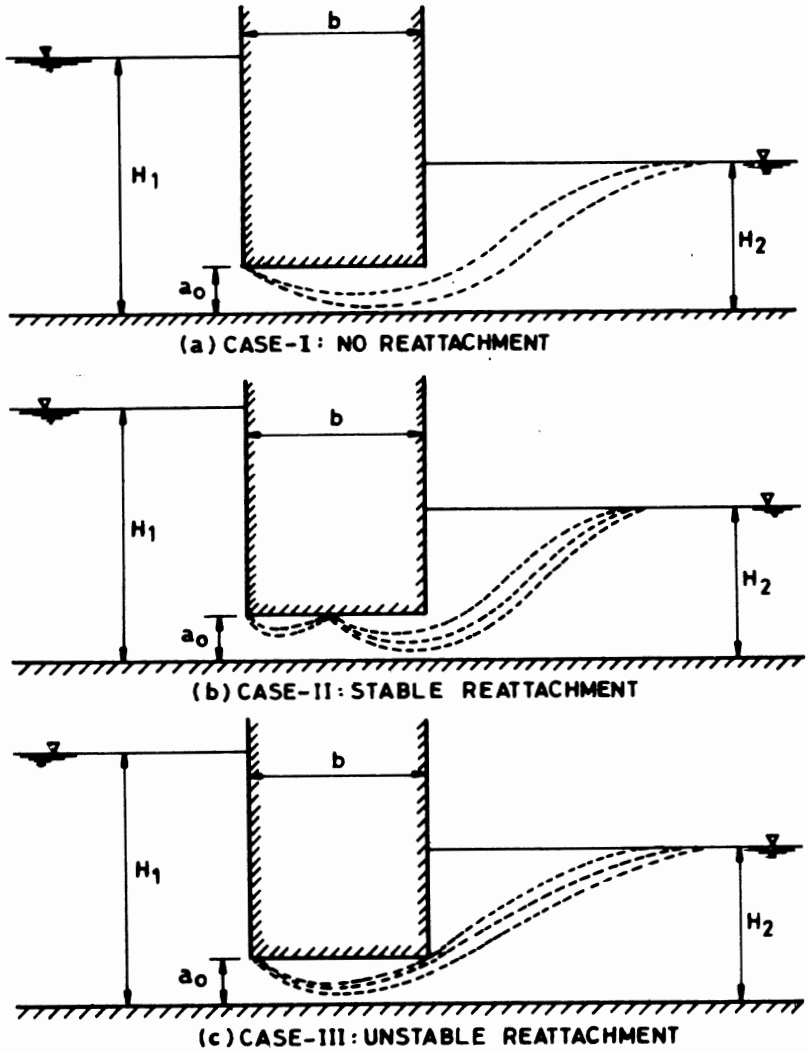

FIG. 1. Schematic diagram of flow behavior below gate showing (a) No-reattachment, (b) Stable reattachment, (c) Unstable reattachment.

In the case of no-reattachment on the gate bottom, less interaction between the resulting shear layer and the gate may take place giving rise to lower intensity of pressure and force fluctuations on the gate bottom. In the stable reattachment case, strong feedback is expected to establish and self-excitation of the gate may generate. In the unstable case, although the feedback is strong, the self-excitation is unstable. The latter two conditions, *i.e.,* stable and unstable reattachment, are important for flat bottom sluice gate.

In the light of the foregoing discussions, a possible parameter describing the geometry of boundaries may be identified as the ratio of the gate bottom thickness to the depth above the gate opening, $b/(H_1-a_o)$, with the notations used in the definition (Fig. 1). Thus, this parameter is believed to serve as a criteria for identifying the different cases of no-reattachment, stable reattachment and unstable reattachment. In this context it may be mentioned that Naudascher and Locher[11] in their studies on flow induced forces on a protruding wall, adopted a parameter b/t, t being the protrusion height, similar to the above parameter which is appropriate for their case of pressure tunnel model. On the other hand, Hardwick[3] in his studies on vertical lift gates, had chosen the gate opening ratio, a_o/b as the criterion for the classification of flow behavior below the gate.

In the absence of the observations on the location of the separation streamlines and the resulting shear layers in this study, it was decided to classify the pressure and force fluctuation data into the three cases, based on the shape of mean pressure distribution diagram or Euler number variation diagram on the gate bottom. The cases for which the Euler number variation on the gate bottom are more or less uniform, are classified as those of no-reattachment, *i.e.,* case I. The runs for which the Euler number variation or mean pressure distribution have peak value near the leading edge of the gate bottom (before the center line) followed by a receding trend are those of stable reattachment, *i.e.,* case II. Lastly, the ones for which the peak Euler number is at or near the trailing edge of the gate bottom (after the center line) are taken as the case of unstable reattachment, *i.e.,* case III and these can be ascertained by experimental evidences only.

2. Experimental Set-up

The experiments conducted in a 10 m long rectangular flume, 0.24 m wide and 0.69 m deep in which water was recirculated through an overhead tank arrangement. The supply pipe to the flume carried a pre-calibrated orifice meter with a manometer for discharge measurements. The test section consisted of proper sized grooves that were provided in the vertical walls of the flume so as to set the gate model with a uniform clearance of 1 mm for the gate to vibrate freely in vertical plane (Fig. 2). A tail gate was provided at the downstream end and pointer gauges were mounted on the flume side walls for depth measurements. All the gate models were 30 cm wide and 30 cm high and made of prespex sheet. The thickness of the hollow gate model were 2.5, 5, 7.5 and 10 cm. Pressure tapping were provided at close intervals on the gate bottom (10 tappings on10 cm thick gate). The tappings were connected through plastic tubing (longest of them being about 90 cm) to an inductive type pressure transducer

with carrier amplifier (KWS/3S-5, HBM, Germany). A gauge well was constructed 1 m upstream of the gate model to connect the pressure transducer at one end by the plastic tube to take advantage of undisturbed upstream water level as reference. It facilitated working with the higher magnitude of the transducer even if the mean pressure at the tapping on the gate bottom was larger and to compute the Euler number. The amplifier signal of the transducer at higher sensitivity was fed to strip chart recorder for the measurement of the pressure fluctuations with sampling time of 50 seconds. The conversion of data from the strip chart recorder into actual pressure fluctuations was carried out using a static calibration of the transducer. The dial reading of the carrier amplifier at low sensitivity gives directly the mean pressure head, $(H_1 - p_x/\gamma)$, p_x being the pressure at the location of the tapping, H_1 is the upstream water level and γ being the unit weight of water. In each run, the upstream and downstream water level, discharge and the gate opening were noted. For gross force measurement on the gate bottom, a strip of 8.5 cm along the gate thickness and 1.5 cm along the width was cut at the gate bottom at the center of the width. A thin phosphor bronze plate 9.8 × 2 cm in size was placed in groove and screwed to the gate bottom such that gate surface was flush with the gate bottom and properly glued to prevent leakage. Two semiconductor strain gauges 10 mm long, 0.25 mm wide and 0.025 m thick with a gauge factor of 95 and nominal resistance of 120 ohms were pasted on the inner surface of the plate, one at its end and another at its center. They were connected to half bridge circuit of universal amplifier and a strip chart recorder. The strain developed in the plate due to hydrodynamic force acting vertically on the plate and transmitted to the semiconductor gauges producing a signal that was amplified and recorded on a chart recorder. The strain strain gauge was precalibrated so that the recorded output could be converted to gross force.

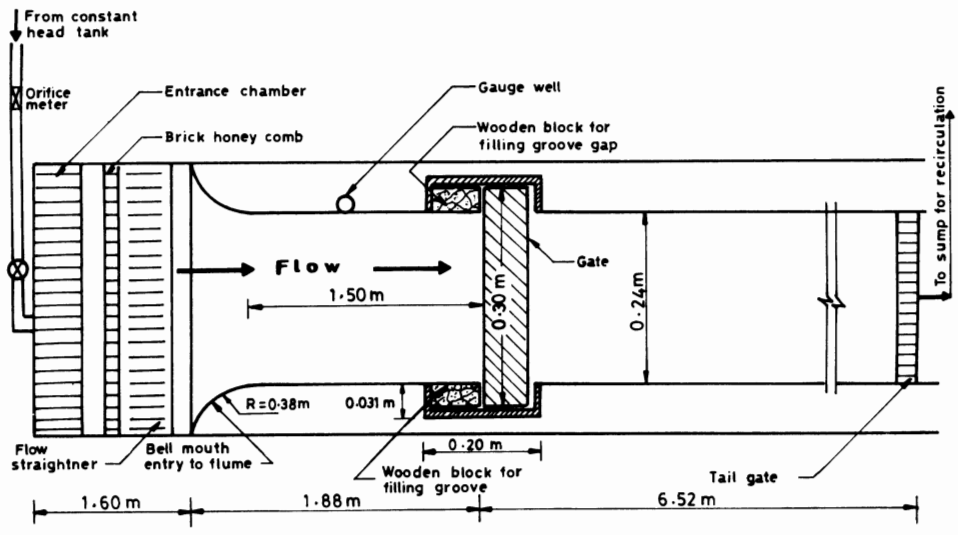

FIG. 2. Plan of experimental set-up (not to scale).

From the records, the mean and the root mean square (RMS) values of the fluctuating components $\bar{p}$ and $\sqrt{\overline{p'^2}}$ of the pressure and $\overline{F}$ and $\sqrt{\overline{F'^2}}$ of force respectively were obtained. The coefficients were computed as follows

$$\overline{C}p_b = \frac{\bar{p} - p_1}{0.5\rho v_1^2} \tag{1}$$

$$\overline{C}F_b = \frac{\overline{F}}{0.5\rho A v_1^2} \tag{2}$$

$$Cp'_b = \frac{\sqrt{p'^2}}{0.5\rho v_1^2}\frac{H_2}{H_1} \tag{3}$$

$$CF'_b = \frac{\sqrt{F'^2}}{0.5\rho A v_1^2}\frac{H_2}{H_1} \tag{4}$$

where $\bar{p}$ is mean pressure intensity at any location on gate bottom, p_1 is reference pressure upstream of gate, v_1 is the velocity of flow under the gate, A is the bottom surface area of the gate, ρ is the mass density of liquid, p' is the fluctuation component of pressure, $\overline{F}$ is the mean gross force, F' is the fluctuating component of force, H_1 and H_2 being upstream and downstream water depth respectively, $\overline{C}_{Pb}$ and C'_{Pb} are mean and fluctuating pressure coefficients, $\overline{C}_{Fb}$ and C'_{Fb} are mean and fluctuating gross force on gate bottom.

3. Discussion of Results

During underflow, the separation of flow from the upstream edge of the gate and subsequent reattachment at location downstream resulted in increased hydrodynamical loading in plane gate vibrations. The mean and fluctuating pressures and gross forces on the gate bottom are dependent on the velocity of water, v_1, gate opening, a_o, gate width, B, gate thickness, b, and location of point x, where the pressure is to be measured. Therefore one could write the following nondimensional equations

$$Cp'_b ; \overline{C}P_b = f_1\left(\frac{x}{b}, \frac{v_1}{\sqrt{a_o g}}, \frac{a_o}{b}, \frac{b}{H_1 - a_o}, \frac{B}{b}, \eta\right) \tag{5}$$

$$CF'_b ; \overline{C}F_b = f_2\left(\frac{v_1}{\sqrt{a_o g}}, \frac{a_o}{b}, \frac{b}{H_1 - a_o}, \frac{B}{b}, \eta\right) \tag{6}$$

in which η refers to the dynamic parameter of the gate, *i.e.*, disturbing force, shaking force and exciting force, ... etc.

3.1 Mean Pressure or Euler Number Variation

The variation of mean pressure coefficient $\overline{C}p_b$ or Euler number E_{nb} with a_o/b, x/b and Froude number, $F_g (= v_1 / \sqrt{(a_o g)})$ was studied. It was noticed that the peak value of $\overline{C}p_b$ occurs close to the upstream edge of the flat bottom gate and decreases with

increasing x/b values as in Fig. 3(a), which may be due to reattachment of flow with the gate bottom. Also it appears that the $\overline{C}p_b$ starts increasing and attains a peak. Its peak value while decreasing shifts slowly towards downstream for increased gate opening ratio, thereby making the distribution more uniform for $a_o/b = 1$. There is no peak of $\overline{C}p_b$ values at all as in Fig. 3(b), this may be due to the absence of reattachment at larger gate openings. It was noted that, $\overline{C}p_b$ has a less dependence on F_g and its value decreased slightly with increasing F_g. It also appears that the pattern of distribution of $\overline{C}p_b$ for stationary gates shows the same trend as for the vibrating one, but the values are somewhat lower. Also, $\overline{C}p_b$ slowly decreases with increase in aspect ratio B/b for a given gate opening ratio.

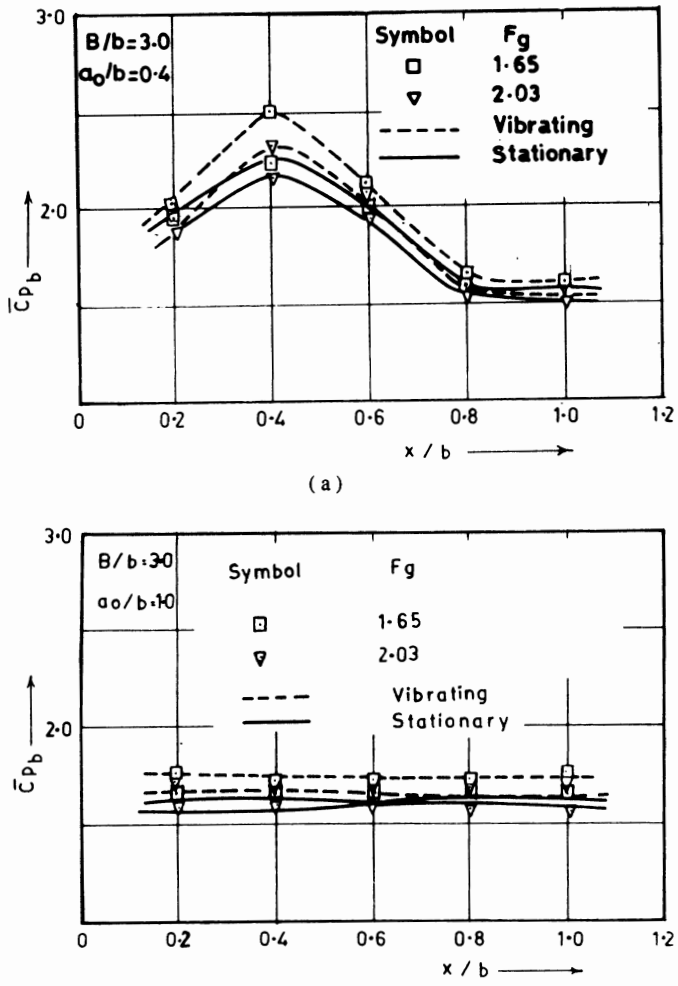

FIG. 3. Typical variation of $\overline{C}p_b$ with x/b on gate bottom for (a) $a_o/b = 0.4$, (b) $a_o/b = 1$, $B/b = 3.0$.

Figure 4 shows the variation of the peak mean pressure coefficient $\overline{C}p_{bm}$ with a_o/b for all the gate models. It is clear that the peak $\overline{C}p_b$ value increases up to a particular gate opening ratio beyond which it decreases and assumes a constant value. For $a_o/b < 0.60$, the peak of $\overline{C}p_b$ is reached indicating the presence of reattachment and for $a_o/b > 0.8$, there is no peak and the distribution of $\overline{C}p_b$ remained fairly constant at large opening ratios, indicating the absence of reattachment. This corroborates fairly well with other authors, Bhargava and Narasimhan[2] and Husain *et al.*[4].

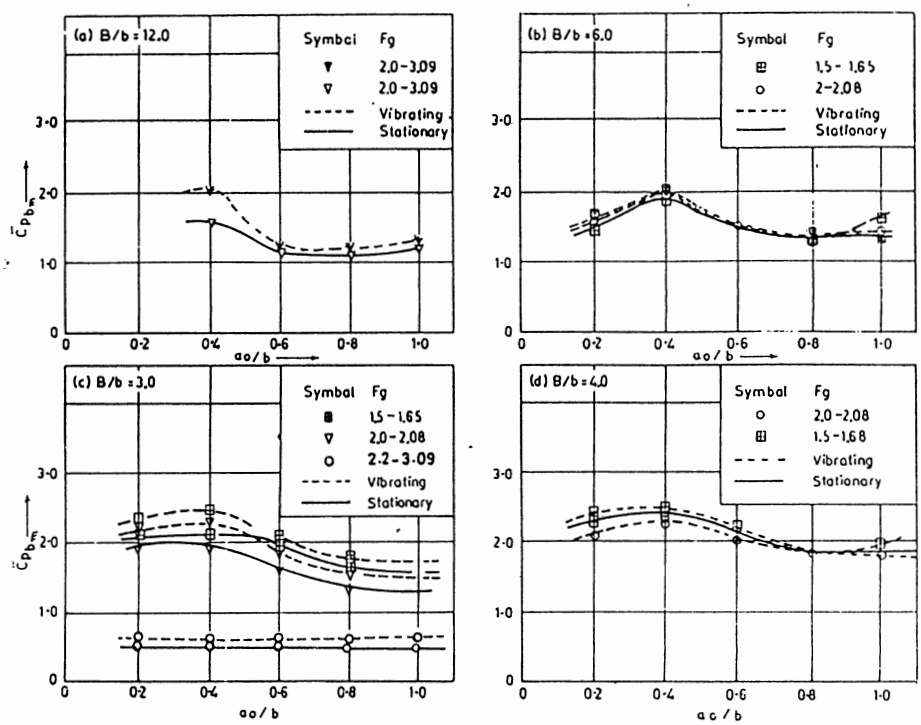

FIG. 4. Variation of $\overline{C}p_{bm}$ on gate bottom with a_o/b for different aspect ratio, B/b.

The shape of mean pressure distribution diagram is shown typically in Fig. 3 & 4. Based on the study of all the pressure distribution data, the following approximate limiting values of $\{ b/(H_1 - a_0) \}$ for the classification of the flow into the different criteria was evolved.

(i) Case I : No reattachment, $b/(H_1 - a_0) < 0.30$.
(ii) Case II : Stable reattachment, $b/(H_1 - a_0) > 0.60$.
(iii) Case III : Unstable reattachment, $0.3 < b/(H_1 - a_0) < 0.60$.

The corresponding values of b/t in the study of Naudascher and Locher[11] are 2.0, 4.5 and between 2.0 and 4.5 respectively, for a tunnel height to protrusion height ratio of 6.0. The difference in the ranges seems to be understandable in view of the large dif-

ference in the blockage ratio of the gate in the present study and protruding wall in that of Naudascher and Locher[11]. In contrast Hardwick[3] identified the limits of $a_0/b > 1.3$, < 0.3 and between 1.3 and 0.3 for the three cases in the order. The difference could be attributed to the possible inadequacy of a_0/b as the criterion for classification.

3.2 Pressure and Force Fluctuations

All the data of the present investigations have been classified according to the criteria laid above. In this subsection, the pressure and force fluctuation data of vibrating and stationary gate have been analyzed in detail in the light of the foregoing classifications.

3.2.1 Variation of Cp'_{bm} with F_g and B/b

The variation of peak value of pressure fluctuation, Cp'_{bm} was already studied against a_0/b and F_g for each value of B/b as shown in Fig. 5 & 6, indicating that the peak Cp'_{bm} occurs at $a_0/b = 0.6$ and decreases assuming a constant value for increased value of $a_0/b > 0.8$, which agrees with the other authors (Bhargava and Narasimhan[2] and Husain *et al.*[4]. Also, the magnitudes of pressure fluctuation are larger for fluctuating gates than the stationary ones. Figure 7 shows the data for Cp'_{bm} versus F_g with B/b as third parameter plotted for the same typical values of gate opening ratios in the case of stable reattachment only. On the figure, tentative dashed lines have been drawn indicating the trend, which demonstrates the prominent influence of Froude number, F_g, and aspect ratio, B/b, on the Cp'_{bm}. It may be noted that Cp'_{bm} is larger at smaller values of B/b for constant value of F_g and a_0/b. Since the gate width, B, was held constant in the present study the behavior mainly signifies the effect of gate thickness on the Cp'_{bm}. This seems understandable since thicker gates have larger bottom area exposed to shear layer and reattaching flows. It is also noted that the lines for different B/b values tend to converge at higher Froude numbers.

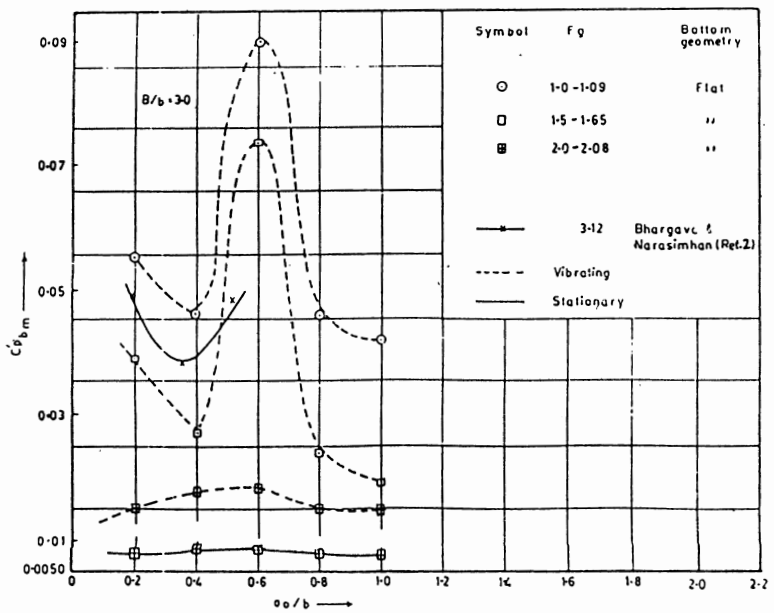

FIG. 5. Variation of Cp'_{bm} on gate bottom with a_0/b for $B/b = 3.0$.

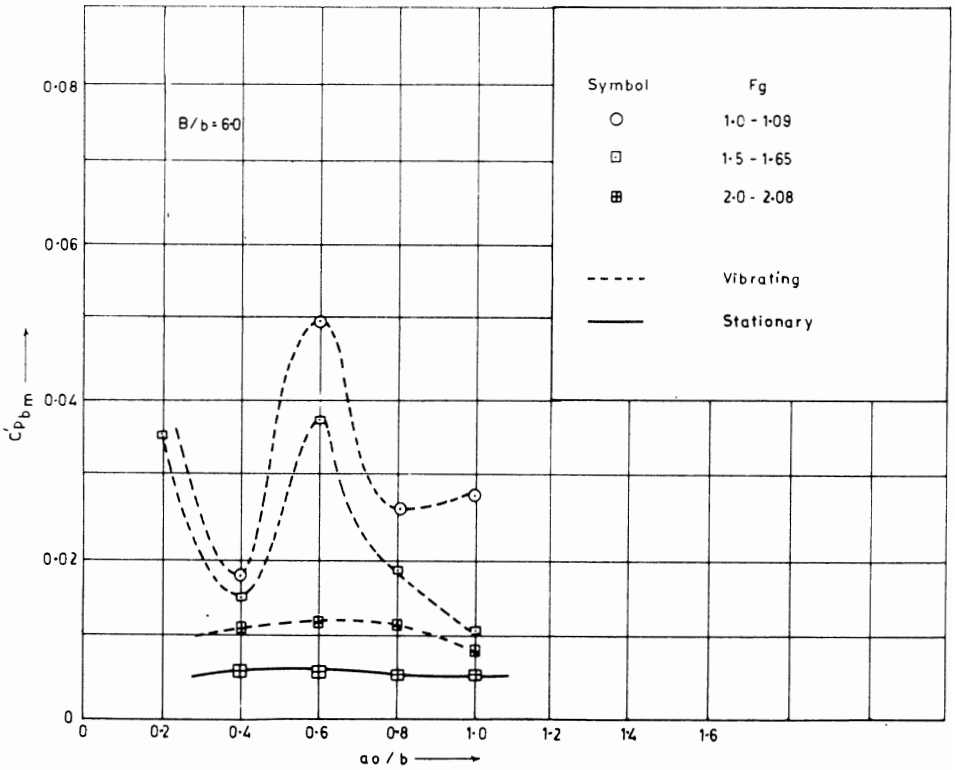

FIG. 6. Variation of on Cp'_{bm} gate bottom with a_0/b for $B/b = 6.0$.

3.2.2 Variation of Cp'_{bm} and CF'_b with Cavitation Parameter (K)

In the study of Naudascher and Locher[11], on a protruding wall in a pressure tunnel, they included a cavitation parameter, $K = (P_1 - P_v)/0.5\ \rho v_1^2$, p_1 and p_v being the mean ambient and vapor pressure respectively along with other parameters which affect the pressure and force fluctuations. They established a criterion $K > 4$ for no cavitation. In an attempt to compare the present data, the values of K were computed and Fig. 8 & 9 show the values of Cp'_{bm} and CF'_b plotted against K for all three cases. As may be seen from these graphs, the values of K for the present data are very high and fall in the range of no cavitation. Further, the data also indicate high intensity of fluctuation for the case of stable reattachment, low intensity for the case of no-reattachment and in between for the case of unstable reattachment. The spread of data in each case is perhaps due to the influence of other parameters like Froude number, aspect ratio, ... etc.

3.2.3 Effect of Self-Excitation on Force Fluctuation

It was noticed by the other investigators that the force fluctuation coefficients, CF'_b are magnified appreciably when the gate is allowed to vibrate and self excite itself[4,6,9,11]. In other words interaction between the flow and gate is much more for a

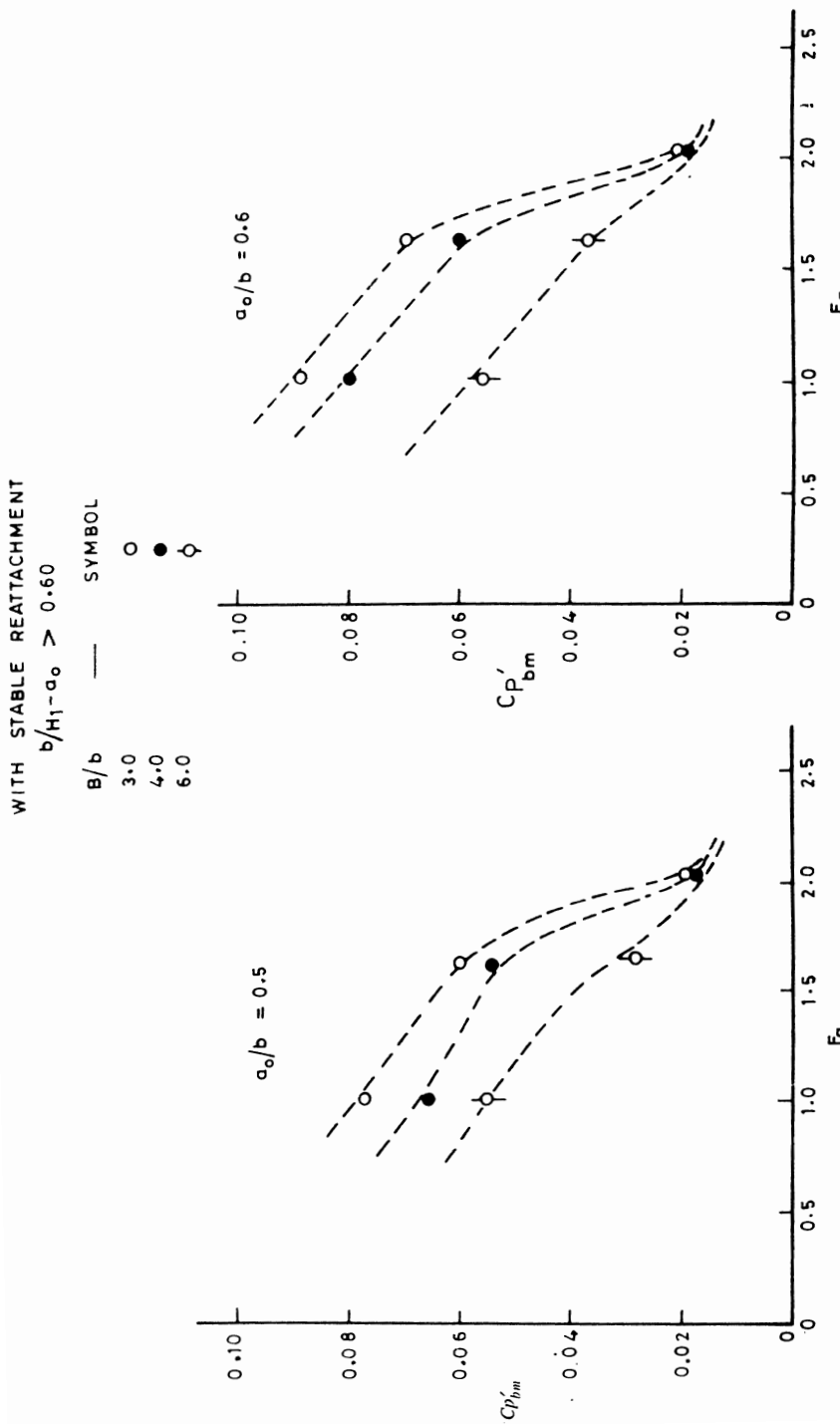

FIG. 7. Typical variation of Cp'_{bm} with F_g for different a_0/b values of 0.5 and 0.6 with stable reattachment case.

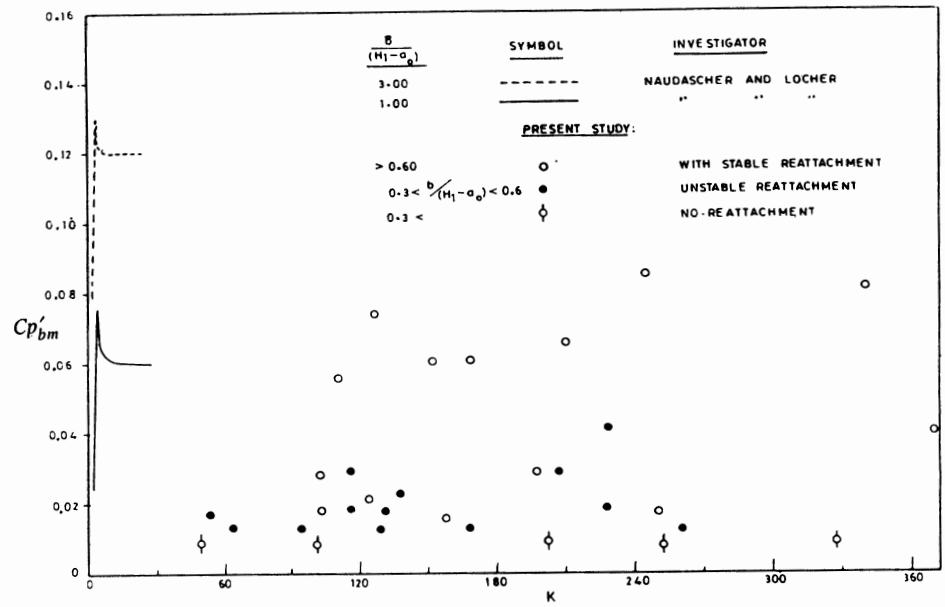

FIG. 8. Variation of Cp'_{bm} with cavitation parameter 'k'.

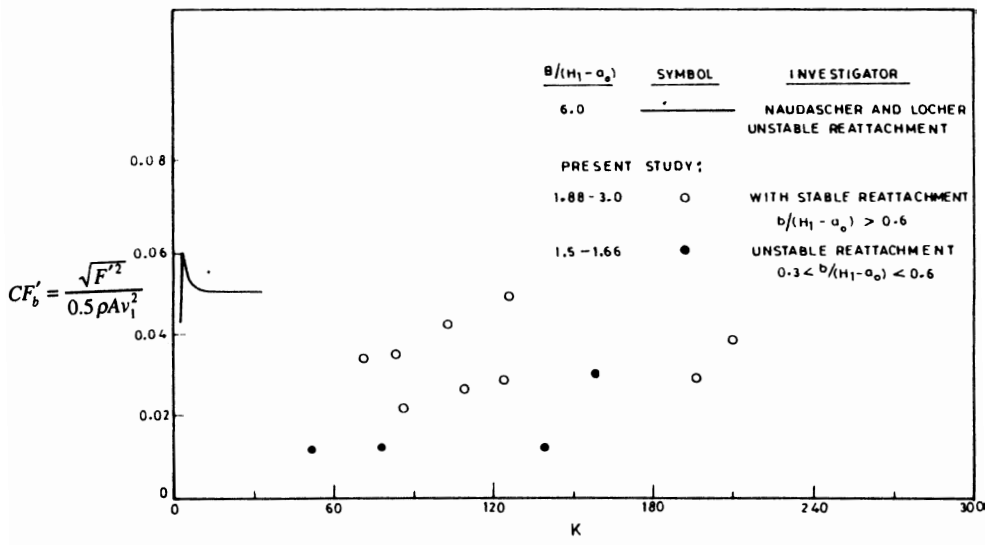

FIG. 9. Variation of CF'_b with cavitation parameter 'k'.

gate allowed to vibrate than for a stationary one. It should be interesting to study the self-excitation effect of gate due to vibration on the value of CF'_b with relevant parameters for the case of stable reattachment, unstable reattachment and no-reattachment. The self-excitation coefficient, C_s(= CF'_b for vibrating gate / CF'_b for stationary gate), of CF'_b has been studied for one gate only. The classification of the underflow gate data as per criterion indicates that most of force fluctuation data fall under the criteria of stable reattachment $\{b/(H_1-a_0) > 0.6\}$. Figure 10 shows a typical variation of C_s with F_g for stable reattachment case, indicating larger value of C_s for low value of F_g. This proves the values of CF'_b is significantly larger for vibrating gates in comparison to stationary ones due to self-excitation when there is a stable reattachment with F_g ranging from 0.5 to 2.5.

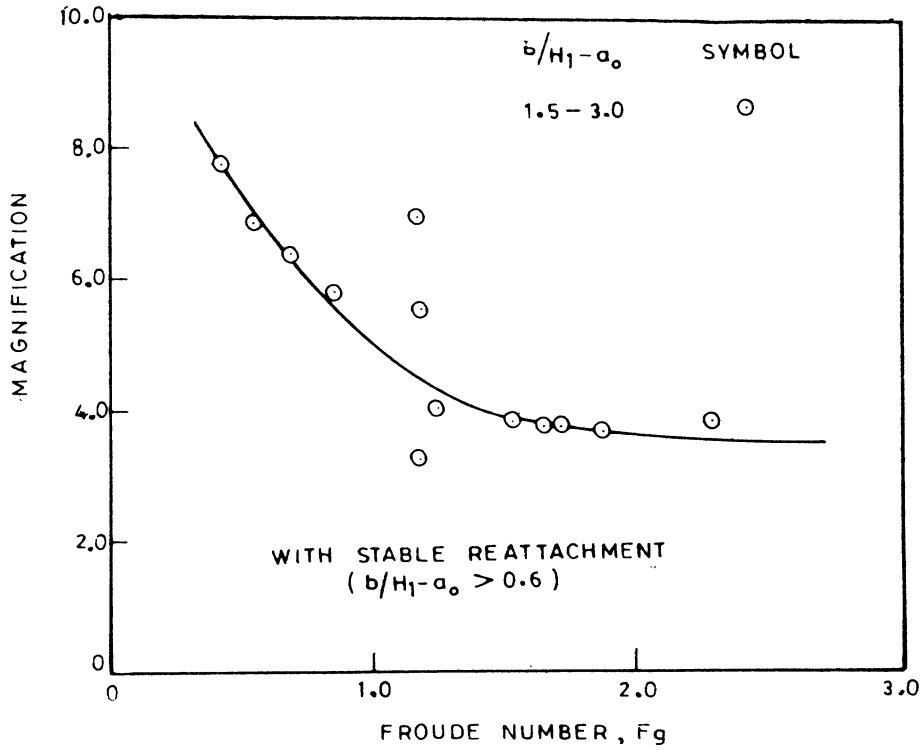

FIG. 10. Typical variation of magnification factor, M, with F_g for B/b = 3.0.

Conclusion

1. Based on mean pressure distribution diagram on gate bottom a criterion has been developed by a parameter, $b/(H_1-a_0)$ with the values of < 0.3, > 0.6 and between 0.3 and 0.6 respectively for identifying the three cases of flow behavior below the gate of no-reattachment, stable reattachment and unstable reattachment.

2. The coefficient of pressure fluctuation, Cp'_b, and force fluctuation, CF'_b, for vibrating gate have been found to be much larger for the case of stable and unstable

reattachment while there is little intensity of fluctuation for the case of no-reattachment.

3. During stable and unstable reattachment the coefficients of force fluctuations were found to be larger for vibrating gates compared to stationary one as a result of self-excitation. The ratio of the fluctuation coefficient for vibrating and stationary gate, *i.e.*, self-excitation coefficient seems to be strongly dependent on Froude number of underflow gates.

References

[1] **Abelev, A.S., Vinogradov, O.G.** and **Dolnikov, L.L. (et. al.),** Structural vibrations due to operation of hydraulic machinery and gates, *Proceedings of 8th Symp. on Hydraulic Machinery, Equipment and Cavitation*, Leningrad, USSR, 6-9 Sept., Paper No. I-1, pp. 3-16 (1976).

[2] **Bhargava, V.P., Narasimhan, S.,** Characteristics of hydrodynamic loading on fixed and vibrating gates, *2nd Int. Symposium on Stochastic Hydraulics, Lund, Sweden, Aug. (1976)*, paper no. 14, 19 p.

[3] **Hardwick, J.D.,** Flow induced vibration of vertical lift gates, *Proc. ASCE, JHD*, **100**(HY5): 631-644 (1974).

[4] **Husain, D., Pande, P.K., Vittal, N.** and **Chandra, R.,** Hydrodynamic loading on vibrating vertical lift gates, *IAHR XX Congress, Sep. 5-9, Moscow*, pp. 346-356 (1983).

[5] **Husain, D.** and **Vittal, N.,** Dynamic response analysis of vibrating vertical leaf gate due to hydrodynamical loading, *First Int. Symp. on Aero-Hydroelasticity, Beijing, China, October 22-23* (1993).

[6] **Husain, D.,** Dynamic study of simultaneous underflow-overflow passed low head sluice gates, *Journal of King Abdulaziz University; Engineering Sciences* (under publishing).

[7] **Kolkman, P.A.,** Analysis of vibration measurements on underflow type of gate, *Proceedings of X Congress, IAHR, London, UK* (1963).

[8] **Kolkman, P.A.,** *Prevention of Self-Excitation Flow Induce Gate Vibration: Prevention of Self Excitation* Ph.D. Thesis, Delft Univ. of Technology, Publication No. 164, Delft Hydraulics Laboratory, Delft, Netherlands (1976).

[9] **Kolkman, P.A.,** Self excited gate vibrations, *Invited Lecture 17th Congress IAHR, Baden-Baden, Germany* (1977); Also Delft Hydraulics Laboratory, Publication No. 186.

[10] **Naudascher, E.,** On the role of eddies in flow induced vibrations, *Proceedings of the 10th Congress, IAHR*, London, Vol. **3:** 61-72 (1963).

[11] **Naudascher, E.** and **Locher, F.A.,** Flow induced forces on protruding walls, *ASCE Proc., Journal of Hyd. Div.*, **100**(Feb.): 295-313 (1974).

[12] **Naudascher, E.,** Flow induced loading and vibration of gates, *Int. Symposium on Hydraulics for High Dams, Beijing, China*, pp. 1-18, Nov. (1988).

[13] **Naudascher, E.,** *Hydrodynamic Forces, IAHR Hydrodynamic Structures Design Manual 3*, AA Balkema, Rotterdam, pp. 247-268 (1991).

[14] **Ogihara, K.,** Hydrodynamic Forces on Moving Gates, *Trans. Japanese Society of Civil Engineers*, Vol. **3** (1971).

[15] **Perkins, J.A.,** Model investigation of the vibration of a vertical lift gate, *Proceedings X Congress IAHR, London, UK*, **3:** 9-16 (1963).

[16] **Petrikat, K.,** Vibration tests on weirs and bottom outlet gates, *Journal of Water Power*, **10**(Feb.): 52-57, (Mar.): 99-104, (Apr.): 147-149, (May): 190-197 (1958).

[17] **Wang, Y.** and **Naudascher, E.,** Scale effects in test on flow induced vibrations I. underflow gates II. Bars and trashracks, *Proc. Symp. on Hydraulic Research in Nature and Lab., Wuhan, China* (1992).

Notations

a_o : gate opening.
b : gate thickness.
B : gate width.
CF' : *coefficient of force fluctuation.*
CF_b : CF on gate bottom.

Cp'	:	pressure fluctuation coefficient.
Cp'_b	:	Cp' on gate bottom.
C_s	:	self-excitation coefficient.
E_{nb}	:	Euler number.
F	:	force.
F_g	:	Froude number.
$f_1 - f_2$	:	functions.
$\overline{F}$	:	mean force.
$\sqrt{\overline{F}'^2}$	:	RMS value of force fluctuation.
g	:	acceleration due to gravity.
H_1, H_2	:	upstream and downstream heads.
m	:	peak value.
p	:	the pressure.
$\overline{p}$	:	the mean pressure
$\sqrt{\overline{p}'^2}$	:	RMS value of pressure fluctuation
v_1	:	velocity under the gate.
x	:	location point of pressure measurement.
γ	:	unit weight of water.
η	:	dynamic parameter.
ρ	:	mass density of fluid.

خاصيـة تحـديد السلوك الدينامي للتدفـق أسفل البوابات المتـذبذبـة

دلوار حسين*، و عبد العظيم محمد نجم، و عبد العزيز عبد الله الحامد***

** قسم الهندسة المدنية ، كلية الهندسة ، جامعة الملك سعود*

الريـــــاض - المملكة العربية السعودية

*** قسم هندسة المياه والمنشآت المائية ، كلية الهندسة ، جامعة الزقازيق - مصر*

المستخلص . يستعرض هذا البحث نتائج الدراسة المعملية عن سلوك التدفق تحت البوابات المتذبذبة ذات القاع المفلطح والمتغير السمك . تم قياس الضغوط والقوى المؤثرة على قاع البوابة أثناء التدفق . واعتماداً على تغير رقم أويلر عند قاع البوابة ، تم استنباط خاصية لتمييز الحالات الثلاث الممكنة لسلوك التدفق تحت البوابة ، من حيث عدم تلامسه مع قاع البوابة أو تلامسه تلامساً مستقراً أو غير مستقر . وتعتمد هذه الخاصية على عمق التدفق قبل البوابة وفتحة البوابة وسمك البوابة .

واستناداً على هذه الخاصية ، فقد تم تحليل بيانات الضغوط والقوى بشكل مفصل . وتبين أن تلامس التدفق مع قاع البوابة يؤدي إلى زيادة التذبذب الذاتي للبوابة ، سواءً أكان هذا التلامس مستقراً أو غير مستقر ، مما يؤدي إلى زيادة التحميل الهيدروديناميي على البوابة .